Correlation effects in Co/Cu and Fe/Cr magnetic multilayers

L. Chioncel[1] and A. I. Lichtenstein[1,2]
[1] *University of Nijmegen, NL-6525 ED Nijmegen, The Netherlands*
[2] *Institut für Theoretische Physik, Universitaet Hamburg, 20355 Hamburg , Deutchland*
(27 May 2003)

Abstract

The electronic structure of Co/Cu(001) and Fe/Cr(001) magnetic multilayers has been investigated within the local density approximation combined with dynamical mean field theory. Our calculation shows enhanced density of states at the Fermi level, suggesting that electronic correlations might play an important role in the transport properties of multilayers.

I. INTRODUCTION

Magnetic multilayers (MML) heterostructures of alternating ferromagnetic layers and non-magnetic spacers have attracted attention in the last decades because of their implications both for fundamental research and technological applications. The most remarkable property of these systems is the giant magnetoresistance (GMR) measured for a parallel/antiparallel configuration of the magnetic moments belonging to different layers in the presence of an external magnetic filed [1]. The GMR effect is related to the spin dependent scattering but the detailed mechanism is still subject of intense investigations.

One of the first attempts to explain the GMR effect was based on the ballistic approach [2]. Soon it became obvious that the band structure description is very important for the realistic description of GMR. A considerable number of attempts have been made to include the electronic structure in diffusive regime [3,4]. In order to consider the spin dependent scattering due to the interface, these calculations were based on the coherent potential approximation. However, all these calculations overestimate the experimental values for the GMR effect. On the other hand band structure calculations allows the evaluation of the Fermi velocities which can be used to estimate the spin dependent relaxation-times [5]. The semiclassical approach used in the calculation of the conductivity overestimate also, the experimental GMR values [6]. One of the most advanced technique in the *ab initio* theories of electric transport in solid systems, is offered by the Kubo-Greenwood formalism. A comprehensive overview of this technique applied for systems with reduced dimension is discussed by Weinberger [7].

In this paper, we demonstrate that the correlations effects might play an important role in the realistic description of transport properties. Our approach is motivated by the fact that the $3d$ transition metal elements, components of the magnetic multilayers, show significant correlation effects. In general, spin-polarized LDA band structure calculation gives an adequate description of the ferromagnetic ground state for the most of metals but, on the other hand, there are obvious evidences of essentially many-body features in photoemission spectra of Fe [8], Co [9], and Ni [10], [11]. The 6 eV satellite in Ni, broadening of the ARPES features due to quasiparticle damping, narrowing of the d-band, essential change of spin polarization near the Fermi level are some examples. It is obvious that these effects can be equally important also for magnetic multilayers and other heterostructures containing transition metals.

II. NUMERICAL DETAILS

We focus on the band structure of the perfect (001) fcc $Co_6/Cu_5/Co_5$ and (001) bcc Fe_3/Cr_5 supercells. It was found experimentally that values of GMR are 220% in Fe/Cr multilayers [12] and 120% in Co/Cu multilayers [13]. One of the reasons why the above multilayers are highly magnetorezistve is that they contain ferromagnetic 3d metals which should have a pronounced spin asymmetry in their conductivity due to the presence of the exchange split d-bands. Perhaps the crucial factors for obtaining high values of GMR are the band matching and the lattice matching between the ferromagnetic

and non-magnetic metals [14,6]. These two conditions are almost perfectly satisfied in Co/Cu and Fe/Cr multilayers. Thin films of Co grow in the fcc structure with the lattice parameter of $3.56\mathring{A}$, which is only 2% less than the lattice parameter of 3.61% in fcc Cu. Both Fe and Cr have the bcc structure and their lattice parameters are almost identical: $2.87\mathring{A}$ for Fe and $2.77\mathring{A}$ for Cr. On the other hand it was experimentally demonstrated that the magnetic multilayers grown epitaxially shows an enhancement of the electronic contribution to the low temperature specific heat [15] which can be an evidence of correlation effects. Indeed, this enhancement cannot be reproduced in the standard electronic band structure calculations [16], probably because of the neglecting of many-body effects. It is our aim to check whether the correlation effects considered in the Dynamical Mean Field Theory (DMFT) [17] approach can lead to an essential renormalization of the density of state at the Fermi level $N(E_F)$.

We performed calculations based on the LDA+DMFT scheme [18]. The present realistic LDA+DMFT method [19] is based on the so-called Exact Muffin-tin orbitals (EMTO) method [20,21] within a screened KKR [22,23], frozen core together with the selfconsistent local spin density approximation (LDA). The correlation effects are treated in the framework of DMFT [17], with the Spin-Polarized T-matrix plus the Fluctuation Exchange (T-FLEX) approximation for the quantum impurity solver [24,25].

In the calculations for the Co/Cu system we considered a tetragonal supercell formed by 16 layers, each layer containg one atom, with an interlayer distance corresponding to the fcc Cu lattice constant $3.61\mathring{A}$. The supercell structure used for the study of the Fe_3/Cr_5 system is presented in Fig. 1. As can be seen the optimization (relaxation) of the atomic layers are neglected, the interlayer distances correspond to the value of the bulk bcc Fe $2.88\mathring{A}$. Each atom type is located on one layer, magnetically symmetric atoms are represented by the same colored spheres. Fe_1 atoms, or interface atoms, are denoted by blue sphere. The central, Fe_2 atoms are indicated by a light blue color. In the picture representing the structure Fig. 1 three extra Fe layers: $Fe_1/Fe_2/Fe_1$ belonging to the next unit cell were introduced. Interface $Cr_{1,2}$ layers are indicated by green, respectively yellow color spheres, meanwhile the central Cr_3 layer is denoted by red sphere. In the calculations the same atomic sphere radius was considered for Fe and Cr in the Fe/Cr, and similarly the radii for Co and Cu atoms were chosen the same for the Co/Cu system.

The $3s, 3p$, and $3d$ states are included for the Co, Cu and Fe valence electrons. In order to calculate the charge density we integrate the Green function along a contour on the complex energy plane which extends from the bottom of the band up to the Fermi level [21], using 30 energy points. For the Brillouin zone integration we sum up a number of 567 k-points for the Co/Cu system and 839 k points for the Fe/Cr respectively. A cutoff of $l_{max} = 8$ for the multipole expansion of the charge density and a cutoff of $l_{max} = 4$ for the wave function was used. The Perdew-Wand [26] parameterization of the local density approximation to the exchange correlation potential was used. Although the lattice mismatch and relaxation have been shown to influence the magnetic properties [27] we neglect this effect.

A. fcc Co and Co/Cu multilayers

We will first discuss the correlation effects on bulk fcc Co, and afterwards investigate the Co/Cu multilayer. The LSDA and LSDA+DMFT density of states for fcc Co is shown in Fig. 2. The LSDA electronic structure of fcc cobalt is different for the majority and minority spin electrons, due to it's ferromagnetism $\mu_{LSDA} = 1.69\mu_B$. DOS can be characterized qualitatively by a shift of the minority and majority d-bands relative to each other. Due to this asymmetry the contributions of the two spin channels to the density of states at the Fermi level will be different, therefore the conductivities are different. This asymmetry in the DOS is the source of GMR in magnetic Co/Cu multilayers. The most important feature of the cobalt DOS is that the Fermi level lies above the top of the d-band for the majority spin electrons.

For the LSDA+DMFT calculations a value of the average Coulomb interaction $U = 2$ eV was chosen. Correlation effects related with spin-flip excitations at non-zero temperature reduce the magnetic moment, $\mu_{DMFT} = 1.42\mu_B$ in comparison with the corresponding LSDA value. The asymmetry between the majority/minority spin channels is kept and an increasing of 12% of DOS at the Fermi level $N(E_F)$ is evidenced. At low energies the majority spin channel presents a satellite structure similar to the one found in the Ni. Due to the perturbation nature of our approach the satellite is shifted towards lower energies.

The energy dependence of the self-energy for Co is plotted in Fig. 3. Near the Fermi level a typical Fermi liquid behavior is evidenced. For the imaginary part $-Im\ \Sigma(E) \propto E^2$, meanwhile the real part of the self-energy has a negative slope $\partial Re\ \Sigma(E)/\partial E < 0$, where E is the electron energy relative to the Fermi level. Due to the fcc structure Co self-energy shows a considerable similarity to the selfenergies of Ni [19]. The high value of the imaginary part of self-energy evidenced around -7eV in the majority spin channel for both t_{2g} and e_g orbitals produce the satellite visible in DOS Fig. 2.

The $Co_6/Cu_5/Co_5$ multilayer, total and the interface layers DOS, in the ferromagnetic orientation are presented in Fig.4. As we seen in Fig. 4, the DOS is asymmetric between the majority and minority spins. In comparison with the bulk fcc Co , Fig. 2, a qualitative description of DOS of $Co_6/Cu_5/Co_5$ can be made, on the base of a "rigid" shift due to the presence of the Cu layers. The Co layers magnetic moment increase as we approach the interface, meanwhile the Cu layers are non-magnetic; the values of the magnetic moments and the electronic specific heat coeficients are presented in table I. The latter is given by the relation $\gamma = \pi^2 k_B^2 N(E_F)(1+\lambda)/3$ where $N(E_F)$ is the electronic DOS at the Fermi level, $(1+\lambda)$ is the mass enhancement factor caused by the electron-phonon interaction. The calculated LSDA+DMFT magnetic moments in the $Co_6/Cu_5/Co_5$ superlattice is shown in Fig. 6, where for comparison we also plot the corresponding quantities obtained using the LSDA. We note that at finite temperatures the Cu layers remain non-magnetic, whereas the value of the magnetic moment on the Co layers diminish in comparison with the LSDA one. Even at finite temperatures $(250K)$ the Co moments couples ferromagnetically across the Co/Cu interfaces.

The energy dependence of the self-energy for the Co interface and central layers are plotted in Fig. 5. Near the Fermi level a typical Fermi liquid behavior is evidenced for both the interface and central Co layers. The imaginary part $-Im\ \Sigma(E) \propto E^2$,

meanwhile the real part of the self-energy has a negative slope $\partial Re\ \Sigma(E)/\partial E < 0$, where E is the electron energy relative to the Fermi level. As can be seen the selfenergies and implicitly the correlation effects are different for the distinct Co layers.

B. bcc Fe, bcc Cr and Fe/Cr multilayers

The correlation effects on bulk bcc Fe, bcc Cr and (001) surface of bcc Fe covered by a trilayer of Cr were described in a previous paper [19]. The present calculations addresses the finite temperature and correlations effects in an eight-layer (3Fe+5Cr) bcc superlattice.

In Fig. 7 the bcc bulk Fe and Cr DOS are presented. As we can see due to the bcc structure the DOS exhibits a pronounced valley in the middle of the d-bands for both spins. Fermi level lies within the d-band for both spin orientations which provides dominance of the d-character. Iron is magnetic $\mu_{LDA} = 2.25\mu_B$, whereas chromium is non-magnetic.

Similarly to the bulk DOS, as it is evident from Fig. 8 the Fermi level in the Fe/Cr system lies within the d-band for both spin orientations. DOS exhibits a pronounced valley for the minority spins with the Fermi level lying almost at the bottom of this valley. This feature of the band structure is a consequence of the similarity of the DOS of minority spin electrons of iron and the minority spin channel DOS of chromium Fig. 7.

Many-body effects described in the framework of the LDA+DMFT, were investigated for different temperatures: $T = 250, 500K$. Since we expect similar correlation effects in the Fe/Cr system the same value of the average Coulomb interaction $U = 2eV$ and the same exchange correlation energy $J = 0.9eV$ was chosen. The DOS for the Fe layers and Cr layers are presented in Fig. 8 and Fig. 10 respectively.

In the case of Fe, Fig. 8 the correlation effects are manifested in a slightly different way for central and interface Fe layers. One can see that for the interface (Fe_1) layer the LSDA peack of the unoccupied DOS close to the Fermi level, is pinned at the Fermi level producing an enhancement of $N(E_F)$. The spectral weight of the main peak in the occupied part ($-1eV$) of spin up channel, is transfered closer to the Fermi level, as temperature is increased. In the same time finite temperature effects smear out the low energy features of DOS, situated in the energy range of $-4, -2$ eV. In the spin down channel, as the correlation effects are switched on a peak at the Fermi level appears. The spectral weight of the $1eV$ spin down LSDA peak is transfered towards the Fermi level and a new peak appears around $0.25eV$. At $T = 250K$, Fig. 8, the weight of the former $1eV$ peak dominates the weight of the $0.25eV$ peak, but as the temperature increases, $T = 500K$, more spectral weight is transfered to the $0.25eV$ peak.

Similarly to the interface Fe_1 layer, the spin down density of states of the central Fe_2 layer show the appearance of the peak at the Fermi level, and the temperature dependence of the spectral weight transfer towards the Fermi level. Due to the correlation effects, the narrowing of the width of the $-1eV$ peak in the spin up channel is evidenced. As the temperature is increased, the $-1eV$ peak shows a slight shift towards the Fermi energy, but it's width is not significantly changed.

The energy dependence of the self-energy for the Fe layers are plotted in Fig. 9. Near the Fermi level a typical Fermi liquid behavior is evidenced for both the interface and central Fe layers. The imaginary part $-Im\ \Sigma(E) \propto E^2$, meanwhile the real part of the self-energy has a negative slope $\partial Re\ \Sigma(E)/\partial E < 0$, where E is the electron energy relative to the Fermi level. As can be seen the selfenergies and implicitly the correlation effects are different for the two distinct Fe layers.

All the above correlation effects can be recognized in the Cr layers as well Fig. 10, in particular the formation of the peak at the Fermi level being a significant feature for the spin down channel. According to the LSDA calculation the density of states of the central Cr layer (Cr_3) is almost the same as that of the bcc Cr bulk Fig.7. As going from the interface Cr layers (Cr_1 and Cr_2) towards the central layer (Cr_3) the spin up channel density of states show the formation of a valley in the DOS near the Fermi level characteristic to the bulk behavior Fig. 10. The interface, Cr_1 layer, DOS is modified appreciable because of the presence of nearby strongly ferromagnetic Fe layer. It is important to note, however that the spin down channel of all Cr layers are not significantly affected by the proximity to the magnetic Fe layer. The spectral weight transfer is also present, but for the interface Cr_1 layer is not that evident since hybridization with the nearby strongly ferromagnetic Fe layer is present.

In Fig. 12 we notice that the magnetic moments of Cr layers alternate from layer to layer and the Fe moments couple ferromagnetically across the Fe/Cr interfaces. According to our LDA+DMFT calculation this Fe/Cr antiparallel coupling across the interface was estimated to be more stable compared to the parallel solution. The temperature dependence of the Fe magnetic moment on each layer is presented in Fig. 13. The central Fe_2 layer follows approximately the behavior of the bulk values, meanwhile the interface layer Fe_1 has a faster temperature decrease. On the other hand the Cr layers show a very peculiar temperature dependence of the magnetic moment due to the couplings across the Fe/Cr layers. Fig. 14 display the Cr layers temperature dependence of the magnetic moment which shows a deviation from the Brillouin function.

The Cr layers being non-magnetic the majority and minority spin self-energies Fig.11 are identical. However correlation effects seems to be more important for the central Cr_3 layer.

III. CONCLUSIONS

The mechanism of giant magnetoresistence in magnetic multilayers is usually related to the spin-dependence of the scattering process. The spin dependent scattering is assumed to arise from spin-dependent random potentials produced by magnetic impurities at the interface or in the bulk of the ferromagnetic layers [34,35]. Recently an improved prediction of the GMR was obtained by combining the disorder effects with the accurate spin-dependent electronic structure calculations [14]. However finite temperature properties and correlations effects were not taken into account.

Several theoretical approaches have been used to explain the magnetic properties of such superlattice structures. Many of these approaches are based on the RKKY-like model [31,32], tight-binding models [33] and, recently, on the results of *ab initio* elec-

tronic structure calculations [29]. The magnetic coupling studied in the framework of these models was shown to result from the interplay between the direct $d-d$ hybridization of Fe and Cr atoms and indirect exchange through the sp electrons. The $sp-d$ coupling [29] was found to be reminiscent of the RKKY interaction only for superlattices with more than four Cr layers [29]. However, for the case of three Cr layers the $sp-d$ coupling model cannot explain the ferromagnetic ordering of Fe atoms.

Based on the theory of spin-fluctuations developed by Moriya [38] and applied by Hubbard [39] for the case of several transition metals, Hasegawa [37] showed that spin-fluctuations plays an important role in discussing the temperature dependence of the GMR. Due to the static approximation employed in the model [37], dynamical effects of the spin-fluctuations were neglected, therefore any definite conclusion on the temperature dependence of GMR were not drawn. Although the explicit calculation of the resistivity and GMR is not the purpose of the present paper, our results include dynamical correlations described in the framework of DMFT [17], being a promising starting point for a direct evaluation of the GMR in multilayer systems.

Using an first principle LDA+DMFT approach [19] we examined the correlation effects and the finite temperature magnetic properties of some Co/Cu and Fe/Cr superlatticels. Our calculations evidenced a peculiar temperature dependence of the magnetic moments near the interface. The correlation effects proved to be different for different atomic layers. Based on the spin polarized T-matrix FLEX, DMFT solver, the correlation effects capture the spin fluctuations that plays primary roles at finite temperatures. Recent experiments on Fe/Cr trilayers showed the existence of magnetic fluctuations [36]. Even though the magnetic excitation were attributed to structural and magnetic disorder in the vicinity of both Fe/Cr interface [36], results presented in this paper suggest that electron-electron interactions give rise to magnetic excitations, which are common features in 3d transition metals systems.

It is worthwhile to emphasize that the enhanced DOS at the Fermi level, having a many-body correlation origin, can play an important role in the GMR, since this DOS enhancement is strongly spin-dependent. It is more effective in the minority channels of Co/Cu And Fe/Cr systems, giving the result of a quasiparticle peak centered at the Fermi level. Our calculation is in good agreement with the tendency of the enhancement of electronic contribution in Fe/Cr magnetic multilayers [15].

ACKNOWLEDGMENTS

L.C. acknowledges the financial supports from: Uppsala University, the "Computational Magnetoelectronics" RTN project (HPRN-CT-2000-00143). This work was supported by the Netherlands Organization for Scientific Research (NWO), grant NWO 047-008-16. Discussions with M.I. Katsnelson, O. Erikksson and I.A. Abrikosov are acknowledged.

REFERENCES

[1] A. Fert, Phys. Rev. Lett. **61**, 2472 (1988); P.Grünberg, Phys. Rev. B **39**, 4828 (1989).

[2] K.M. Schep, P. J. Kelly and G.E.W. Bauer, Phys. Rev. Lett. **74** , 568 (1995).

[3] W.H. Buttler, J.M. MacLaren and X.G. Zhang, Mater. Res. Soc. Symp. Proc. **313**, 59 (1993).

[4] R.K. Nesbet, J. Phys. Condens. Matter **6**, L449, (1994).

[5] P. Zahn, I. Mertig, M. Richter and H. Eschrig Phys. Rev. Lett. **75**, 2996 (1995).

[6] E.Yu. Tsymbal and D.G. Pettifor, J. Appl. Phys **81**, 4579 (1997); Solid State Phys **56**, 113 (2001).

[7] P. Weinberger, Physics Reports-Review Section of Physics Letters, **377**, 281 (2003).

[8] M. I. Katsnelson and A. I. Lichtenstein J. Phys. Condens. Matter **11**, 1037, (1999).

[9] S. Monastra et al, Phys. Rev. Lett. **88**, 236402 (2002).

[10] A. I. Lichtenstein, M. I. Katsnelson, and G. Kotliar, Phys. Rev. Lett. **87**, 067205 (2001).

[11] M. van Schilfgaarde, V.P. Antropov, J. Appl. Phys. **85**, 4827 (1999).

[12] R.Schad, C.D. Potter, P. Belien, G. Verbach, J. Dekoster, G. Langouche, V.V. Moschalkov and Y. Bruynseraede, J. Magn. & Magn. Mater., **148**, 331 (1995); R.Schad, C.D. Potter, P. Belien, G. Verbach, V.V. Moschalkov and Y. Bruynseraede, Appl. Phys. Lett., **64**, 3500 (1994).

[13] S.S.P. Parkin, Z.G. Li and D.J. Smith, Appl. Phys. Lett., **58**, 2710 (1991).

[14] E.Yu. Tsymabl and D.G. Pettifor, J. Phys. Condens. Matter **8**, L569, (1996).

[15] B. Revaz el al., Phys. Rev. B **65**, 094417 (2002).

[16] N. I. Kulikov and C. Demangeat, Phys. Rev. B **55**, 3533 (1997).

[17] A. Georges, G. Kotliar, W. Krauth, and M. J. Rozenberg, Rev. Mod. Phys. **68**, 13 (1996).

[18] V. I. Anisimov, A. I. Poteryaev, M. A. Korotin, A. O. Anokhin, G. Kotliar, J. Phys.: Condens. Matter **9**, 7359 (1997); A. I. Lichtenstein and M. I. Katsnelson, Phys. Rev. B **57**, 6884 (1998).

[19] L. Chioncel, L. Vitos, I. A. Abrikosov, J. Kollár, M. I. Katsnelson, and A. I. Lichtenstein, Phys. Rev. B. **67**, 235106 (2003).

[20] O. K. Andersen, O. Jepsen, and G. Krier, in *Lectures on Methods of Electronic Structure calculations*, edited by V. Kumar, O.K. Andersen, and A.Mookerjee (World Scientific Publishing Co., Singapore, 1994), p. 63; O. K. Andersen and T. Saha-Dasgupta, Phys. Rev. B **62**, R16219 (2000).

[21] L. Vitos, H. L. Skriver, B. Johansson, and J. Kollár, Comp. Mat. Sci. **18**, 24 (2000); Phys. Rev. B **29**, 179 (2001).

[22] P. Weinberger, in *Electron scattering theory for ordered and disordered matter* (Clarendon Press, Oxford, 1990).

[23] J.R. Taylor, *Scattering Theory: The Quantum Theory of Non-relativistic collision* (Robert E. Krieger Pub. Comp, 1983).

[24] M. I. Katsnelson and A. I. Lichtenstein, Eur. Phys. J. Phys. B. **30**, 9 (2002).

[25] A.I. Lichtenstein and M. I. Katsnelson, in *Band Ferromagnetsim. Ground State and Finite-Temperature Phenomena*, edited by K. Barbeschke, M. Donath, and W. Nolting, Lecture Notes in Physics (Springer-Verlag, Berlin, 2001), p. 75.

[26] J. P. Perdew and Y. Wang, Phys. Rev. **45**, 13244 (1992).
[27] R. Wu and A.J. Freeman, Phys. Rev. B **51**, 17131 (1995).
[28] S. Mirbt, I. A. Abrikosov, B. Johanson and H. L. Skriver Phys. Rev. B **55**, 67 (1997).
[29] K. Ounadjela et al, Europhys. Lett. **15**, 875 (1991).
[30] J. Landes et al, J. Magn. & Magn. Mater., **86**, 71 (1990).
[31] Y. Yafet, J. Appl. Phys. **61**, 4085 (1987).
[32] Y. Wang, P.M. Levy, and J.L. Fry, J. Magn. & Magn. Mater. **93**, 395 (1991).
[33] D. Stoeffler and F. Gautier, Prog. Theor. Phys. Suppl. **101**, 139 (1990).
[34] P.M. Levy, S. Zhang and A. Fert, Phys. Rev. Lett., **65**, 1643 (1990).
[35] H. Itoh, J.Inoue and S. Maekawa, Phys. Rev. B, **51**, 342 (1995).
[36] E. Kentzinger, U. Rucker, B. Topereverg, Th. Bluckel, Physica B **335**, 89 (2003).
[37] H.Hasegawa and F. Herman, Phys. Rev. B, **38**, 4863 (1988); H.Hasegawa, Phys. Rev. B, **47** 15080 (1993).
[38] *Spin fluctuations in Itinerant Electron Magnetism*, edited by T.Moriya (Springer, Berlin, 1985).
[39] J. Hubbard, Phys. Rev. B, **19**, 2626 (1979); **20**, 4583 (1979); **23**, 5970 (1983).
[40] N. E. Phillips, Crit. Rev. Solid. State Sci. **2**, 467 (1971).
[41] E. Fawcett, Rev. Mod. Phys. **60**, 209 (1988).

TABLES

TABLE I. Theoretical magnetic moments μ and electronic specific heat coeficients γ calculated for bulk bcc Fe, Cr and fcc Co. The experimental values for γ include the contribution from the electron-phonon coupling, which is not included in the results obtained from band structure calculations. In the last three columns, the parameters used in the self-consistent LSDA+DMFT calculations are listed.

	μ_{LDA} (μ_B)	μ_{DMFT} (μ_B)	γ_{LDA} $(mJ/K^2\ mol)$	γ_{DMFT} $(mJ/K^2\ mol)$	γ_{exp} $(mJ/K^2\ mol)$	T (K)	U (eV)	J (eV)
Co	1.62	1.38	5.43	6.78	-	250	2	0.9
Fe	2.25	2.24	2.43	2.61	3.11,3.69[a]	250	2	0.9
Cr	-	-	1.73	2.40	3.5[b]	250	2	0.9

[a] Ref. [40]

[b] Non-magnetic Cr, Ref. [41].

TABLE II. The calculated magnetic moments in the LSDA (T=0K) and LSDA+DMFT (T=250K) for the $Co_6/Cu_5/Co_5$ superlatice.

	μ_{LDA} (μ_B)	$\mu_{DMFT}(T=250K)$ (μ_B)	U (eV)	J (eV)
$Co_1(Co/Cu)$	1.44	1.12	2.0	0.9
$Co_2(Co/Cu)$	1.44	1.02	2.0	0.9
$Co_3(Co/Cu)$	1.37	1.04	2.0	0.9
$Co_4(Co/Cu)$	1.31	1.06	2.0	0.9
$Co_5(Co/Cu)$	1.31	1.09	2.0	0.9
$Co_6(Co/Cu)$	1.35	1.20	2.0	0.9
$Cu_1(Co/Cu)$	0.00	0.02	0.0	0.0
$Cu_2(Co/Cu)$	0.00	0.00	0.0	0.0
$Cu_3(Co/Cu)$	0.00	0.00	0.0	0.0

TABLE III. Temperature dependence of layer resolved magnetic moments. The bulk values of the magnetic moment for the same temperatures, and the parameters used in DMFT calculations are presented in the table.

	μ_{LDA} (μ_B)	$\mu(T=250K)$ (μ_B)	$\mu(T=500K)$ (μ_B)	U (eV)	J (eV)
$Fe(bulk)$	2.25	2.24	2.21	2.0	0.9
$Fe_1(Fe/Cr)$	1.97	1.78	1.70	2.0	0.9
$Fe_2(Fe/Cr)$	2.54	2.38	2.42	2.0	0.9
$Cr_1(Fe/Cr)$	-0.54	-0.04	-0.08	2.0	0.9
$Cr_2(Fe/Cr)$	0.43	0.05	0.04	2.0	0.9
$Cr_3(Fe/Cr)$	-0.45	-0.18	-0.16	2.0	0.9

FIGURES

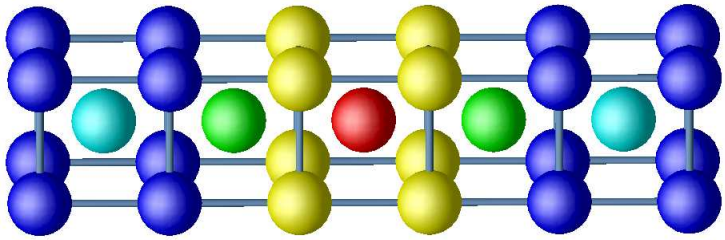

FIG. 1. The superlattice strcuture of Fe_3/Cr_5 having an equidistant distribution of atomic layers. Fe atoms are denoted by blue spheres and Co atoms are indicated by green yellow and red sphere, in the following order: $Fe_1/Fe_2/Fe_1/Cr_1/Cr_2/Cr_3/Cr_2/Cr_1/Fe_1/Fe_2/Fe_1$. The tetragonal supercell is formed by the first 8 atomic layers (3Fe+5Cr) aligned along the z direction.

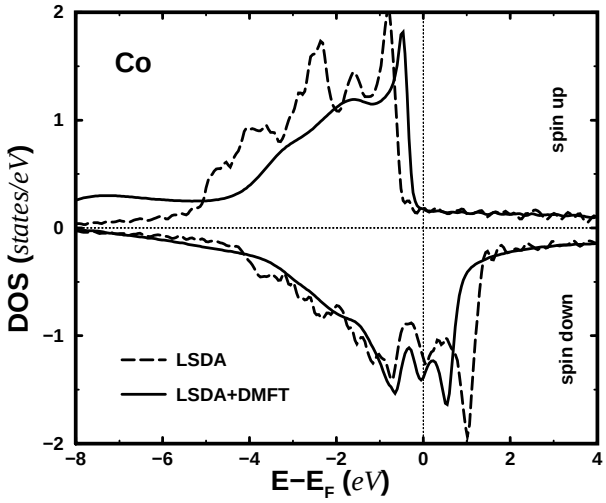

FIG. 2. The LSDA (dashed line) and LSDA+DMFT (solid line) densities of states for fcc Co calculated using the EMTO-DMFT method. A significant reduction of the exchange splitting can be evidenced.

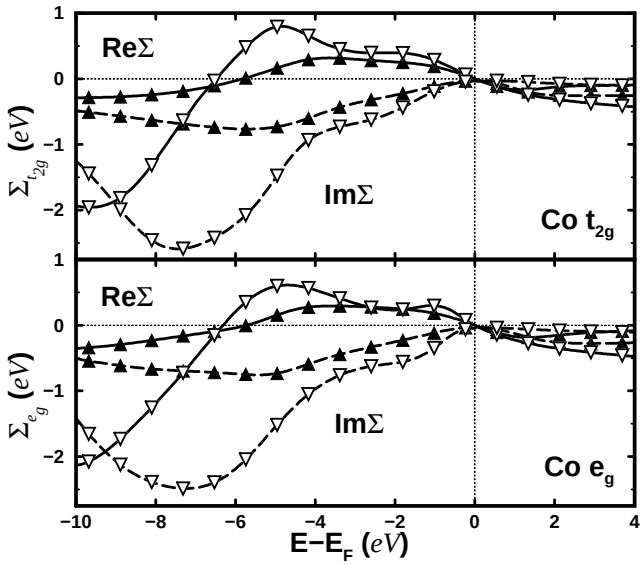

FIG. 3. Spin up (open symbols) and down (closed symbols) self energies for fcc Co for t_{2g} (upper panel) and e_g (lower panel) orbitals.

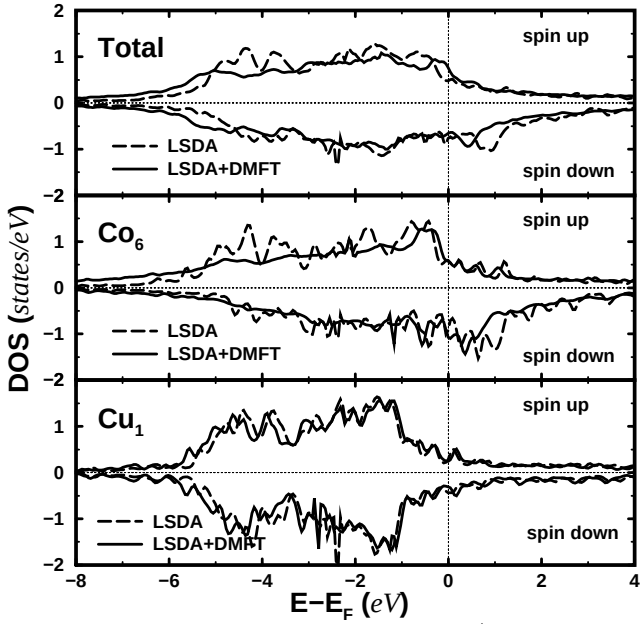

FIG. 4. Total DOS and the interface layers Co_6/Cu_1 LSDA (dashed line) and LSDA+DMFT (solid line) densities of states.

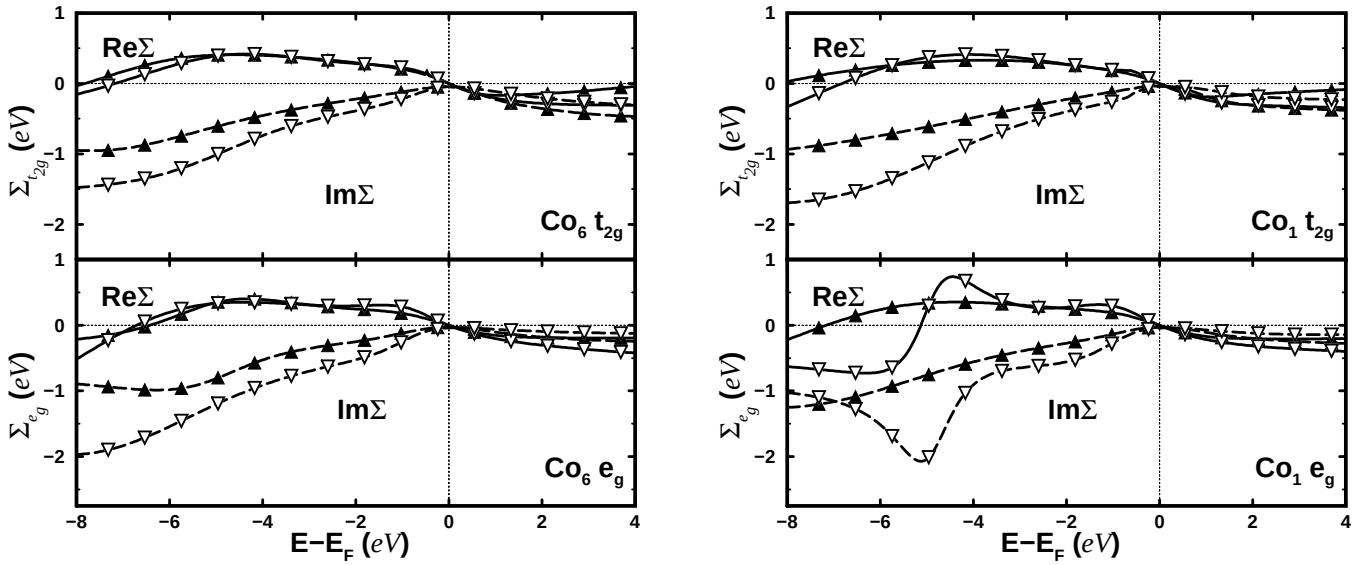

FIG. 5. Layer resolved self-energies: Co_6-interface layer and Co_1 - central layer at temperature $T = 250$.

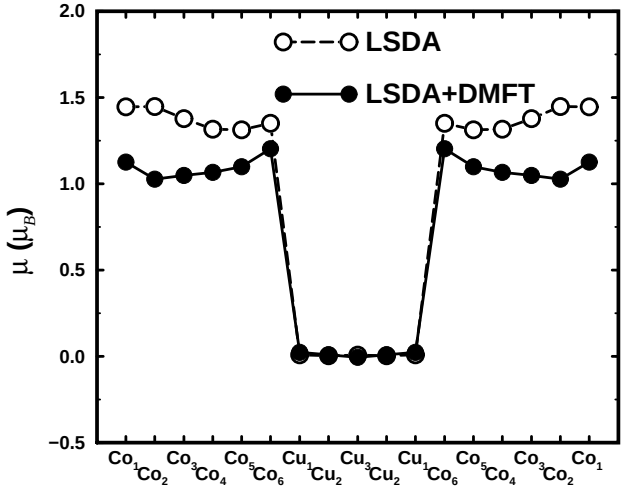

FIG. 6. Distribution of the layer resolved magnetic moment at T=0K (LSDA) and T=250K (LSDA+DMFT) in Co/Cu superlattice.

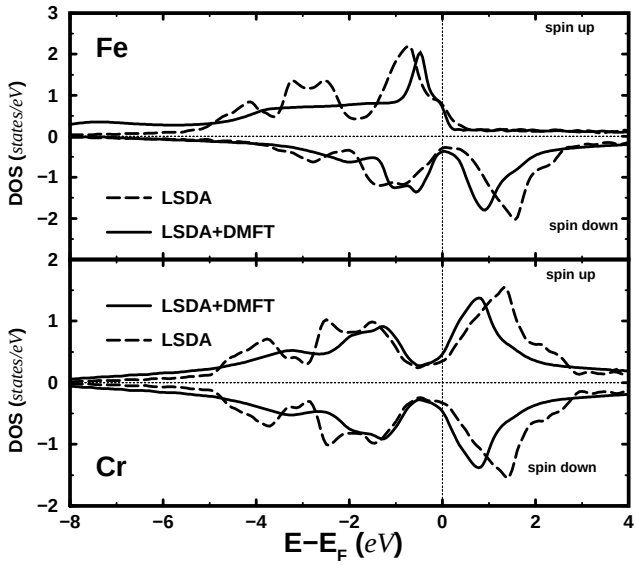

FIG. 7. Bulk bcc iron and chromim DOS, LSDA (dashed line) and LSDA+DMFT (solid line). The similarities of DOS in the minority spin channel determines the minority spin channel behaviour of Fe_3/Cr_5 multilayers.

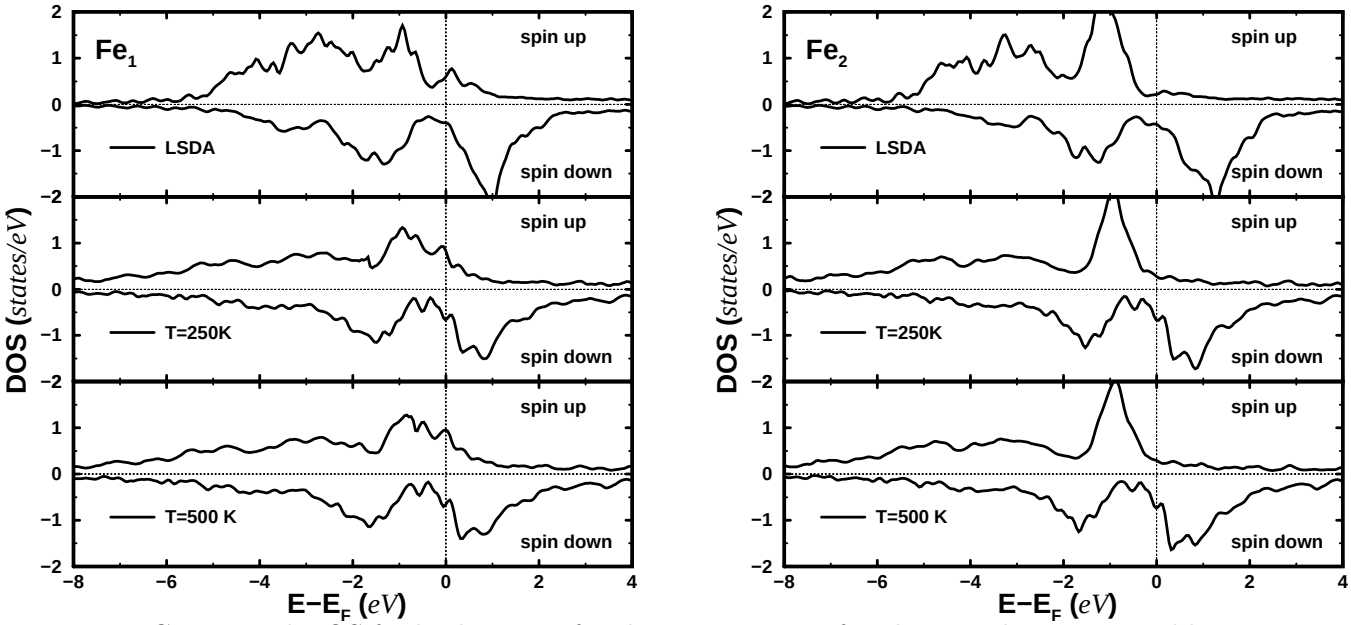

FIG. 8. Total DOS for both types of Fe layers: Fe_1-interface layer and Fe_2 - central layer. The temperature dependence of DOS is presented for $T = 0, 250$ and $500K$ respectively.

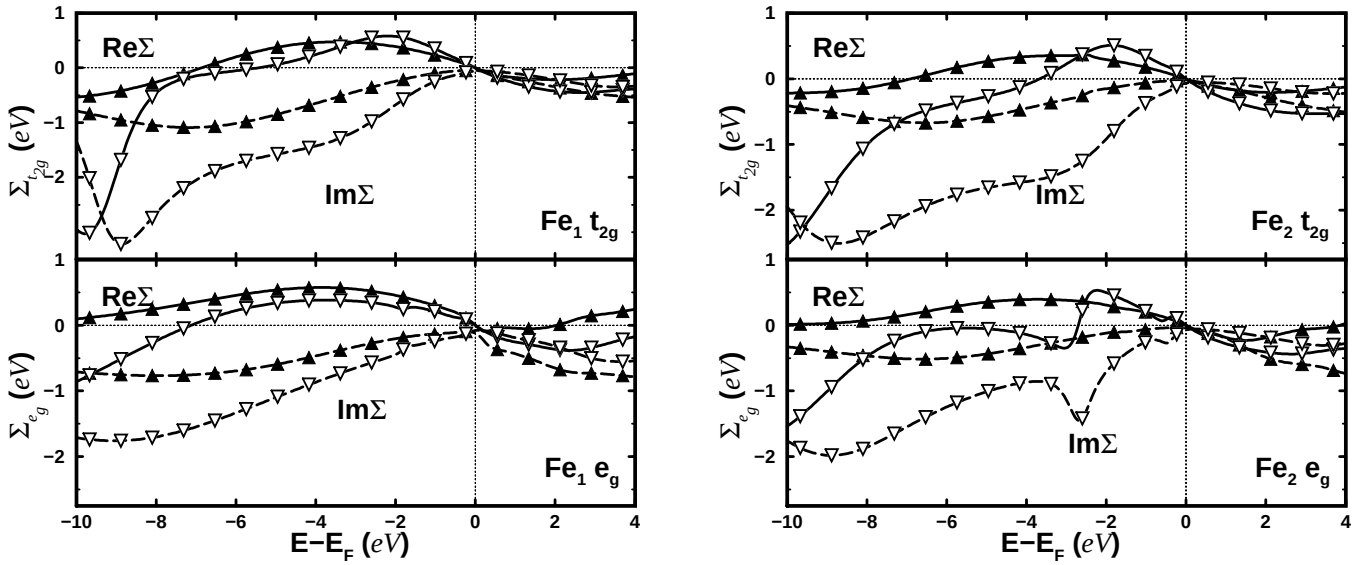

FIG. 9. Layer resolved self-energies: Fe_1-interface layer and Fe_2- central layer at temperature $T = 500$.

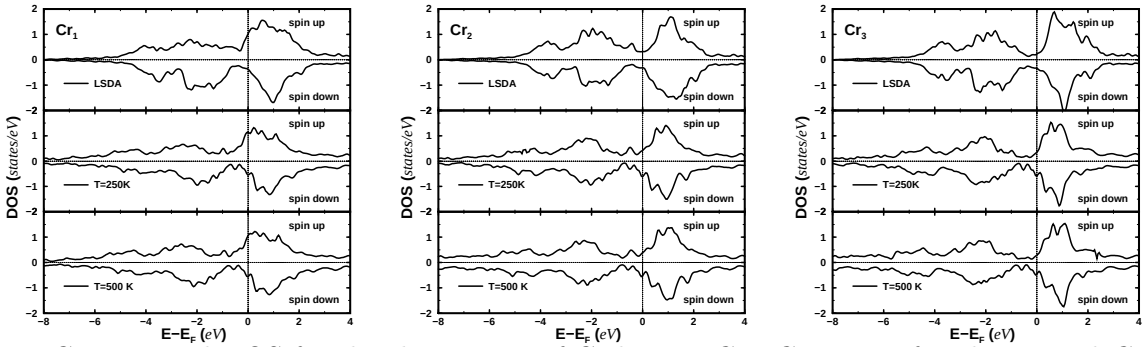

FIG. 10. Total DOS for the three types of Cr layers: Cr_1, Cr_2 - interface layers and Cr_3 - central layer. The temperature dependence of DOS is presented for $T = 0, 250$ and $500K$ respectively.

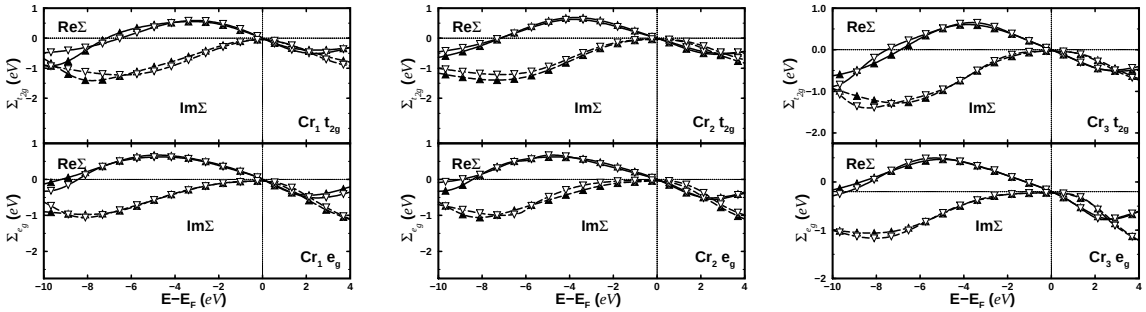

FIG. 11. Layer resolved self-energies for Cr layers: Cr_1, Cr_2 - interface layers and Cr_3 - central layer for for $T = 500$.

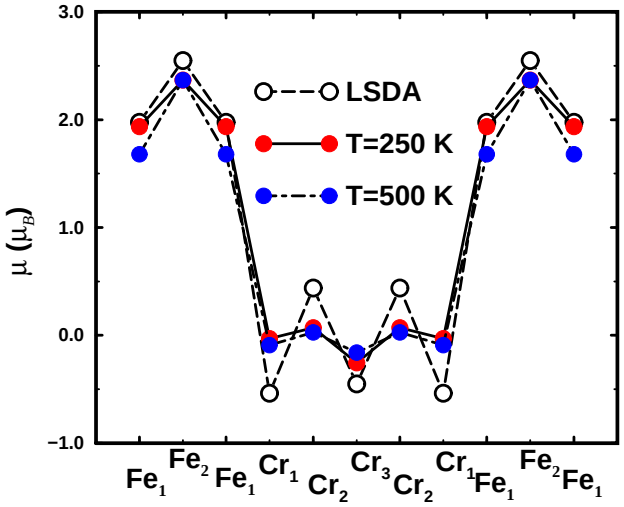

FIG. 12. The distribution of the local magnetic moments at T=0, 250 and 500K in 3Fe +5 Cr superlattice as given by the LSDA and the different DMFT calculations

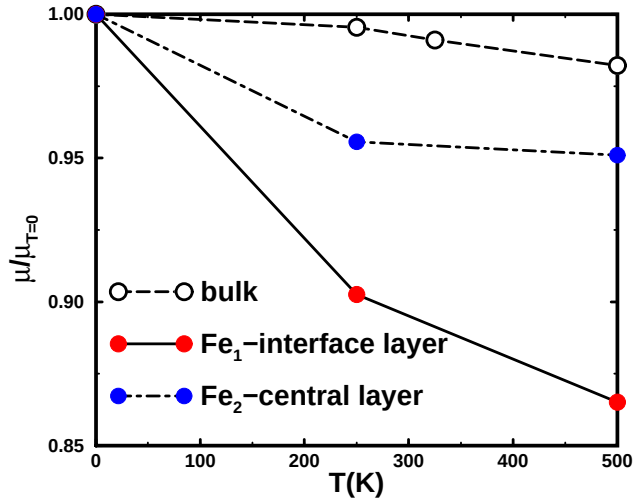

FIG. 13. Temperature dependence of the calculated magnetic moments on the Fe layers is presented in comparison the temperature dependence of the calcualted bulk bcc Fe magnetic moments. The value at $T = 325K$ is taken from the reference [19]. The normalization of the magnetic moment is done with respect to the LSDA value ($\mu_{T=0}$).

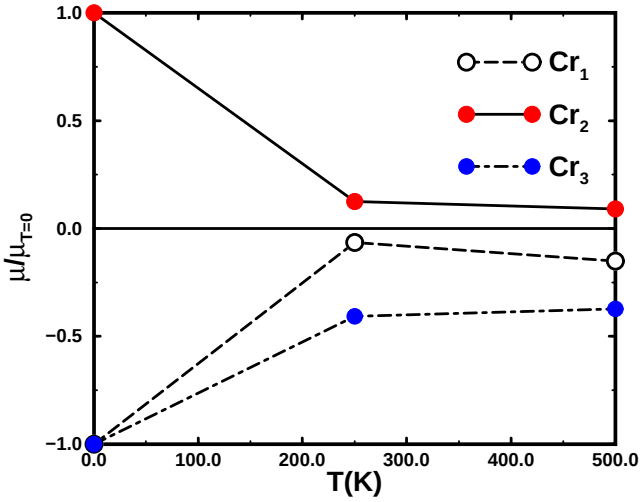

FIG. 14. Temperature dependence of the magnetic moment on the Cr layers. The normalization of the magnetic moment is done with respect to the LSDA value ($\mu_{T=0}$).